Available online at www.sciencedirect.com
ScienceDirect

Journal of Computational Physics 226 (2007) 732–753

JOURNAL OF COMPUTATIONAL PHYSICS

www.elsevier.com/locate/jcp

Accelerated Cartesian expansions – A fast method for computing of potentials of the form $R^{-\nu}$ for all real ν

B. Shanker [a,*], H. Huang [a,b]

[a] Department of Electrical and Computer Engineering, Michigan State University, 2120 Engineering Building, East Lansing, MI 48824, United States
[b] Department of Physics and Astronomy, Michigan State University, East Lansing, MI 48824, United States

Received 17 November 2006; received in revised form 23 April 2007; accepted 26 April 2007
Available online 14 June 2007

Abstract

The need to compute potentials of the form $R^{-\nu}$ for $\nu \geqslant 1$ occur in a variety of areas ranging from electromagnetics to biophysics to molecular dynamics to astrophysics, etc. For instance, Coulomb, London, Lennard-Jones, H-bonds are of the form $\nu = 1, 5, 6$ (and 12), 10, respectively. For a systems with N source/observation points, the cost of computing these potentials scales proportional to $\mathcal{O}(N^2)$. Methods to overcome this computational bottleneck have been a popular research topic for quite some time. For instance, the fast multipole method (FMM) and their cousins—tree codes—have revolutionized the computation of electrostatic potentials ($\nu = 1$). These methods rely on a hierarchical decomposition of the computational domain, i.e, construction of a regular oct-tree decomposition, and exploits the principle of divide and conquer to compute potentials at each observation point. This paper presents two methods, in the vein of FMM, albeit based on Cartesian tensors. The salient features of the first are as follows: (i) it relies on totally symmetric tensors and (ii) the errors are *independent* of the height of the tree. The second method is presented specifically for $\nu = 1$, and relies on *traceless* totally symmetric Cartesian tensors. Using the relationship between traceless Cartesian tensors and spherical harmonics, it will be shown that this technique has the same computational cost as the classical FMM. Generalization of the second method for $\nu \neq 1$ is trivial; however, one needs to use totally symmetric tensors instead. Finally, in the whole computation scheme, only the translation operator (that used to traverse across the tree) depends on ν. Convergence of the proposed method is proven for all $\nu \in \mathbb{R}$. Numerical results that validate the cost and accuracy are presented for several potential functions; these include those typically encountered in the analysis of physical systems (Coulombic, Lennard-Jones, Lattice gas).

1. Introduction

Computation of pairwise interaction (for instance, Columbic interactions, London potentials, or Van der-Wall's potential, etc.) is important in numerous research areas that are as diverse as biophysics, physics, computation chemistry, astrophysics, and electrical engineering to name a few. For example, $\nu = 1, 5, 6, 10$

[*] Corresponding author. Tel.: +1 517 432 8136; fax: +1 517 353 1980.
E-mail address: bshanker@egr.msu.edu (B. Shanker).

0021-9991/$ - see front matter © 2007 Elsevier Inc. All rights reserved.
doi:10.1016/j.jcp.2007.04.033

corresponds to Columbic interactions/gravitational potentials, London dispersion potentials, van der Waals potentials, and H-bonds, respectively. However, it is well known that computing these potentials requires prohibitive computation resources, both in terms of CPU cycles and memory. These costs are exacerbated when such computation is required either in a molecular dynamics or a Monte Carlo setting. It is well known that the CPU cost of computing mutual interactions between N particles distributed in $\mathbb{R}^3$ scales as $\mathcal{O}(N^2)$. Consequently, this has engendered the need for computational methodologies that are efficient both in terms of memory and CPU time. Some of these include cutoff techniques [1], particle mesh algorithms [2–4], Ewald summation (based on an assumption of periodicity) [5,6], tree-codes [7–9] and fast multipole methods (FMM) [10–13]. Tree codes (and FMM) are based on subdividing the computational domain into hierarchical subdomains, and computing the influence between subdomains that are sufficiently separated using multipole/local expansions. The fundamental differences between FMM and tree codes notwithstanding, these methods have revolutionized analysis in application domains ranging from astrophysics to biophysics to engineering sciences.

At this point, we note that there is rampant confusion in terminology; in fact, the terms FMM and tree codes are used interchangeably in the literature that we have come across. This is not surprising as the two techniques are closely related. The differences between these two methods, albeit subtle, are significant. As was elucidated in [14], tree codes compute interactions between source pairs using one of three methods: (i) directly, (ii) evaluating fields at each observation point using multipole expansion due to a cluster of sources, or (iii) using local expansion at observation clusters to find fields. The decision on the operation used depends on which one is computationally efficient. On the other hand, the algorithmic structure of FMM enables the computation of potentials in an optimal manner [14]. Two addition operations that permit this are aggregation and disaggregation functions. These permit the computation of information at coarser (or finer) using information at finer (or coarser) levels. It so happens that for $v = 1$, tree codes typically rely on Cartesian expansions, whereas FMM is based on spherical harmonics. In this paper, we develop theorems and operations necessary for constructing FMM methods ($\forall v$) using Cartesian tensors.

Tree codes for computing the Lennard-Jones potential was developed as early as 1996 [15]. More refined methods for computing the same were proposed by [16–18]. All three methods essentially use Taylor's expansion in the Cartesian coordinates, and some of these use Gegenbauer polynomials based recursion techniques to accelerate translation of multipole expansion to fields at the observer. In 2005, [19] proposed a variation of these schemes using Taylor's series expansion in a different coordinate systems. Other techniques that have been proposed rely on precorrected fast Fourier transform and using a singular value decomposition. Developing FMM-like techniques using special functions has proven difficult [19] as Gegenbauer polynomials in the spherical coordinate system are not separable. However, it is well known that Gegenbauer polynomials can be written in terms of Legendre polynomials. Sarin et. al. used this fact to develop a tree code; since Legendre polynomials are used, an FMM scheme may be readily derived from these expressions as well. Recently, Chowdry and Jandhyala [20] developed operators necessary to extend their scheme to a multilevel setting. However, using Gegenbauer polynomials for either recursion or developing tree codes has a singular disadvantage; these polynomials are defined for $v \geqslant -1/2$. Consequently, methods that rely explicitly on these cannot be generalized to non-oscillatory potentials (like the lattice gas potential) nor can one prove convergence $\forall v \in \mathbb{R}$.

The motivation for writing this paper are fourfold: (i) To formulate a fast method for $1/R^v$ in terms of *totally* symmetric tensors, and exploit these to reduce the costs. (ii) To introduce new theorems that enable *exact* traversal up and down the tree. This implies that one *does not* accrue error as the height of the tree increases. (iii) To prove convergence $\forall v \in \mathbb{R}$. (iv) To demonstrate the intimate connection between the classical FMM introduced by Greengard [10] and its Cartesian counterparts using traceless Maxwell Cartesian tensors. This connection will show that properly constructed Cartesian FMM schemes have the same computational complexity as classical FMM. Another salient feature of the proposed method is that it can readily form the framework for rapidly computing potentials that are non-oscillatory (e.g. Lattice gas, Yukawa, Gauss Transform, Lattice Sums, etc.) without the use of special functions (application of this methodology to some of these potentials will be presented elsewhere). Furthermore, this algorithm is capable of aggregating different potentials within the same simulation tree.

Development in fast methods for computing Columbic interactions ($v = 1$) have progressed along two fronts: exploiting the representation of the potential using either spherical harmonics or Taylor's expansions. The latter was introduced at approximately the same time as the Greengard's first paper on three-dimensional FMM [21], and has found extensive application in tree-codes. Recently, FMM codes based on Cartesian expansions have used recurrence relations to avoid derivatives [22]. Typically, asymptotic computational cost of schemes based on Cartesian expansions is higher. This is because spherical harmonics are optimal for representing harmonic functions in three dimensions. For a system with N mutually interacting particles, it can be readily proven that for a one-level implementation, the computational complexity scales as $\mathcal{O}(P^4N)$ and $\mathcal{O}(P^6N)$ for FMMs based on spherical harmonics and Cartesian expansions, respectively. Here, P is the number of harmonics used in the computation. This cost can be reduced by choosing the number of particles at the lowest level in the tree in an optimal manner. Our interest in revisiting these schemes is motivated by the following observations: (i) Taylor's series expansions provides a natural framework for developing addition theorems [23]; (ii) Taylor's expansion involves representing the fields in terms of Cartesian tensors; (iii) there is an intimate connection between Cartesian tensors and the spherical harmonics. These connections are well known, and have been explored extensively (as early as Maxwell!); see [24–26] and references therein. The following statements hold true: (i) components of a traceless tensor of rank n serve as constant coefficients in a spherical harmonic of degree n, and (ii) there is a class of traceless tensors of rank n whose components are n-degree spherical harmonics functions of x, y, z. These connections imply that there should be an intimate connection between the two seemingly disparate methodologies, and one should be able to obtain a similar cost structure for both methods. As we will show, the recurrence relationship that were *conjectured* for translating multipole expansions [22] can be rigorously derived using traceless tensors. This implies that one should be able to derive a computational scheme using Cartesian tensors that are optimal in the sense of FMM. The method presented herein can be readily generalized to analyze potentials for all v or, for that matter, to any potential function whose power series converges rapidly [27] (for instance, the Yukawa potential), and more importantly, without the need to use special functions!

Thus, this paper will focus on the use of Cartesian tensors to derive fast computational schemes for all v. Similar to classical FMMs, the methodologies developed herein will rely on a divide and conquer computational strategy that is facilitated by a hierarchical partitioning of the computational domain through the construction of an oct-tree data structure. The underlying mathematics for two different computational methods will be derived; in the first, operators will be derived for traversing up, down and across the tree. This technique will rely on using totally symmetric tensors. The salient feature of this method is that the traversal up and down the tree (or shifting the origin of the multipole/local expansion) is exact. The second method produces optimal technique, in the sense of FMM, for $v = 1$. This optimality is achieved using *traceless* totally symmetric tensors. For $v \neq 1$, it yields the same computational complexity as the first, albeit a different error bound. One of the most interesting features of both algorithms, which separates the proposed technique from [28], is the fact that the operators derived for traversing up and down the tree are *independent* of v, and only traversing across the tree depends on v. This is a powerful feature, as one can use a single traversal up and down the tree to compute the combined effects of different potentials! Finally, the algorithm presented does not involve *any* explicit (or numerical computation of) derivatives, and quantities are expressed in terms of (products of) traceless (or totally symmetric) tensors.

This paper is organized as follows: in Section 2 we will present relevant details and theorems regarding tensors, detracer, Maxwell Cartesian tensors, and homogeneous polynomials. Here, we also demonstrate the intimate connection between traceless tensors and Legendre polynomials. In Section 3, we present the two FMM-like algorithms, implementation details, and computational cost. In Section 4, we present numerous results to validate the accuracy and to demonstrate the efficiency of the proposed method. Finally, in Section 5, we summarize the contribution of this paper.

2. Preliminaries

This section introduces basic notation and theorems that will be used in the rest of this paper. The material presented builds upon some of the earlier work by Applequist [26,29,30]. For completeness, we have described some of the theorems given in his papers (without proofs) as well as added some of our own (with the necessary proofs).

2.1. Tensors

A Cartesian tensor $\mathbf{A}^{(n)}$ of rank n is an array of 3^n components and will also be denoted either in component notation as $A^{(n)}_{\alpha_1\cdots\alpha_n}$ where $\alpha_j \in \{1,2,3\}$. A totally symmetric tensor is one that is independent of the permutation of indices $\alpha_1\cdots\alpha_n$; in compressed form it contains $(n+1)(n+2)/2$ independent components, and is denoted by $A^{(n)}(n_1,n_2,n_3)$ where $n_1+n_2+n_3=n$. Here, n_i is the number of times the index i is repeated. For example, consider the direct product of the vectors $\underbrace{\mathbf{rr}\cdots\mathbf{rr}}_{n\text{ times}} = \mathbf{r}^n$. It forms a tensor of rank n (and will be referred to henceforth as a polyadic) whose component can be expressed in compressed form as $r^{(n)}(n_1,n_2,n_3)=x^{n_1}y^{n_2}z^{n_3}$. The trace of one index pair of a tensor results in a tensor of rank $n-2$ and is denoted by $\mathbf{A}^{(n:1)}_{\alpha_3\cdots\alpha_n} = \mathbf{A}^{(n)}_{\nu\nu\alpha_3\cdots\alpha_n}$; the superscript $(n{:}\mu)$ indicates a trace in μ index pairs, and will result in a tensor of rank $n-\mu-1$. If the trace vanishes for any index pair then the tensor is totally traceless. It follows from the above description that if a tensor is symmetric and traceless in one index pair, then it is traceless for all index pairs.

2.2. Tensors contraction

Consider two tensors $\mathbf{A}^{(m+n)}$ and $\mathbf{B}^{(n)}$. The n-fold contraction between these two tensors is given by $\mathbf{A}^{(m+n)}_{\beta_1\cdots\beta_m\alpha_1\cdots\alpha_n}\mathbf{B}^{(n)}_{\alpha_n\cdots\alpha_1}$, and will be denoted using $\mathbf{C}^{(m)} = \mathbf{A}^{(m+n)}\cdot n\cdot\mathbf{B}^{(n)}$. As usual, repeated indices denote a summation over that index. Similarly, a direct product between two tensors $\mathbf{A}^{(n)}$ and $\mathbf{B}^{(m)}$ results in a tensor of rank $n+m$. If $\mathbf{A}^{(n+m)}$ and $\mathbf{B}^{(n)}$ are two totally symmetric tensors, then the n-fold contraction between them can be written in compressed notation as

$$\begin{aligned}
&\mathbf{C}^{(m)} = \mathbf{A}^{(n+m)}\cdot n\cdot\mathbf{B}^{(n)}\\
&C^{(m)}(m_1,m_2,m_3) = \sum_{n_1,n_2,n_3}\frac{n!}{n_1!n_2!n_3!}A^{(n+m)}(n_1+m_1,n_2+m_2,n_3+m_3)B^{(n)}(n_1,n_2,n_3)
\end{aligned}\tag{1}$$

It is evident that the number of operations involved in evaluating each term of the tensor $C^{(m)}(m_1,m_2,m_3)$ is $(n+1)(n+2)/2$, and since there are $(m+1)(m+2)/2$ terms, the total cost of the above contraction is $(m+1)(m+2)(n+1)(n+2)/4$. Next, we consider contraction between a totally symmetric tensor and two other tensors.

Theorem 2.1. *In evaluating an* $(n+m)$*-fold contraction between a totally symmetric rank* $\mathbf{C}^{(n+m)}$ *tensor and two tensors of* $\mathbf{B}^{(n)}$ *and* $\mathbf{A}^{(m)}$ *it is permissible to permute the order of contraction. In other words*

$$\mathbf{A}^{(m)}\mathbf{B}^{(n)}\cdot(n+m)\cdot\mathbf{C}^{(n+m)} = \mathbf{B}^{(n)}\mathbf{A}^{(m)}\cdot(n+m)\cdot\mathbf{C}^{(n+m)}$$

Proof. The proof is best derived in component form. The tensor $\mathbf{C}^{(n+m)}$ is totally symmetric, and a permutation of any pair of indices does not alter the value of the tensor. Carrying this procedure between pairs of indices of the tensor $\mathbf{C}^{(n+m)}$ results in $C^{(n+m)}_{\beta_1,\ldots,\beta_n,\alpha_1,\ldots,\alpha_m} = C^{(n+m)}_{\alpha_1,\ldots,\alpha_m,\beta_1,\ldots,\beta_n}$. Thus,

$$\begin{aligned}
\mathbf{A}^{(m)}\mathbf{B}^{(n)}\cdot(n+m)\cdot\mathbf{C}^{(n+m)} &= A^{(m)}_{\alpha_1,\ldots,\alpha_m}B^{(n)}_{\beta_1,\ldots,\beta_n}C^{(n+m)}_{\beta_1,\ldots,\beta_n,\alpha_1,\ldots,\alpha_m} = B^{(n)}_{\beta_1,\ldots,\beta_n}A^{(m)}_{\alpha_1,\ldots,\alpha_m}C^{(n+m)}_{\alpha_1,\ldots,\alpha_m,\beta_1,\ldots,\beta_n}\\
&= \mathbf{B}^{(n)}\mathbf{A}^{(m)}\cdot(n+m)\cdot\mathbf{C}^{(n+m)} \qquad \square
\end{aligned}\tag{2}$$

Finally, we note a trivial fact that will be useful in generating methods with lower computational complexity.

Lemma 2.2 (Non-uniqueness). *Let* $\mathbf{A}^{(n)},\mathbf{B}^{(n)}$ *and* $\mathbf{C}^{(n)}$ *be full rank tensors. Then it follows that if* $\mathbf{A}^{(n)}\cdot n\cdot\mathbf{B}^{(n)} = \mathbf{C}^{(n)}\cdot n\cdot\mathbf{B}^{(n)}$, *it implies that either* $(\mathbf{A}^{(n)}-\mathbf{C}^{(n)})\perp_n\mathbf{B}^{(n)}$ *or* $\mathbf{A}^{(n)} = \mathbf{C}^{(n)}$ *where* $\perp_n$ *defines an n-fold orthogonality.*

2.3. Homogeneous polynomials

Consider a vector $\mathbf{r} \in \mathbb{R}^3$ and a homogeneous polynomial $f(\mathbf{r})$ of degree n. The following lemma [30] prescribes the relation between homogeneous polynomials and the polyadic $\mathbf{r}^n$.

Lemma 2.3. *A polynomial of nth degree is homogeneous if and only if it can be written as*

$$f_n(\mathbf{r}) = \mathbf{A}^{(n)} \cdot n \cdot \mathbf{r}^n \tag{3}$$

where $\mathbf{A}^{(n)}$ *is an nth rank Cartesian tensor that is independent of* $\mathbf{r}$.

The proof for this lemma may be found in [26]. The following observations are also in order:

(1) The polyadic $\mathbf{r}^n$ is totally symmetric. This implies that one can recast (3) as $f_n(\mathbf{r}) = \mathbf{A}^{(n)}_{\mathrm{sym}} \cdot n \cdot \mathbf{r}^n$ where the symmetric tensor $\mathbf{A}^{(n)}_{\mathrm{sym}}$ is related to the tensor $\mathbf{A}^{(n)}$. This fact implies that a homogeneous polynomial can *always* be represented in terms of symmetric tensors.
(2) The above expression can also be interpreted as a projection of an nth rank tensor along the vector $\mathbf{r}$.
(3) If the tensor $\mathbf{A}^{(n)}$ is totally symmetric and the n-fold contraction with $\mathbf{r}^n$ vanishes, i.e., $\mathbf{A}^{(n)} \cdot n \cdot \mathbf{r}^n \equiv 0$, then each component of $\mathbf{A}^{(n)}$ vanishes. The proof for this assertion can be found in [26].

Next, the Gradient and Euler's theorems are as follows:

Theorem 2.4. *If* $f_n(\mathbf{r})$ *is a homogeneous polynomial, i.e,* $f(\mathbf{r}) = \mathbf{A}^{(n)} \cdot n \cdot \mathbf{r}^n$, *then*

$$\nabla^k f_n(\mathbf{r}) = \frac{n!}{(n-k)!}\mathbf{A}^{(n)} \cdot (n-k) \cdot \mathbf{r}^{n-k} \quad (k \leqslant n) \tag{4}$$

Theorem 2.5. *If* $f_n(\mathbf{r})$ *is a homogeneous polynomial of degree* $n \geqslant 0$, *then*

$$\mathbf{r}^k \cdot k \cdot \nabla^k f_n(\mathbf{r}) = \frac{n!}{(n-k)!} f_n(\mathbf{r}) \quad (k \leqslant n) \tag{5}$$

In both these equations, and hereafter, the tensor operator $\nabla^n = \underbrace{\nabla \cdots \nabla}_{n}$. The proofs for these theorems can be found in [26]. Likewise, it can be shown that if $\mathbf{A}^{(n)}$ is totally traceless, then $f_n(\mathbf{r})$ is a solid spherical harmonic of degree n. This fact will be used extensively to construct operators with low computational complexity.

2.4. Detracer

As seen in the previous subsection, a homogeneous polynomial can be represented in terms of a contraction of a polyadic with a traceless tensor. Obtaining a traceless tensor from a totally symmetric tensor is tantamount to projecting out an nth rank irreducible tensor [31,32]. In what follows, we shall use the detracer operator that has been used for constructing Cartesian tensorial forms of spherical harmonics [26]. Formally, the detracer operator is defined as $\mathscr{D}_n$, which, when acting on a totally symmetric tensor $\mathbf{A}^{(n)}$, results in a traceless totally symmetric tensor. More specifically, this operation is defined as

$$\mathscr{D}_n A^{(n)}_{\alpha_1\cdots\alpha_n} = \sum_{m=0}^{\lfloor \frac{n}{2} \rfloor} (-1)^m (2n-2m-1)!! \sum_{T\{\alpha\}} \delta_{\alpha_1\alpha_2} \cdots \delta_{\alpha_{2m-1}\alpha_{2m}} A^{(n:m)}_{\alpha_{2m+1}\cdots\alpha_n} \tag{6a}$$

where the sum over $T\{\alpha\}$ is a sum over all permutations of $\alpha_1 \cdots \alpha_n$, and $n!!$ denotes the double factorial of n. If $\mathbf{A}^{(n)}$ is expressed in compressed form, the same equation can be rewritten as

$$\mathscr{D}_n A^{(n)}(n_1,n_2,n_3) = \sum_{m_1=0}^{\lfloor \frac{n_1}{2} \rfloor} \sum_{m_2=0}^{\lfloor \frac{n_2}{2} \rfloor} \sum_{m_3=0}^{\lfloor \frac{n_3}{2} \rfloor} (-1)^m (2n-2m-1)!! \begin{bmatrix} n_1 \\ m_1 \end{bmatrix} \begin{bmatrix} n_2 \\ m_2 \end{bmatrix} \begin{bmatrix} n_3 \\ m_3 \end{bmatrix} \times A^{(n:m)}(n_1-2m_1, n_2-2m_2, n_3-2m_3) \tag{6b}$$

where $n = n_1 + n_2 + n_3, m = m_1 + m_2 + m_3$, and

$$\begin{bmatrix} n \\ m \end{bmatrix} = \frac{n!}{2^m m!(n-2m)!} \tag{6c}$$

Note, that a traceless totally symmetric tensor of rank n has only $2n + 1$ independent components. Some interesting properties associated with the Detracer (and the proofs for the theorems that follow) can be found in [29,30] are as follows:

Theorem 2.6 (Exchange theorem). *If* $\mathbf{A}^{(n)}$ *and* $\mathbf{B}^{(n)}$ *are totally symmetric tensors, then*

$$\mathbf{A}^{(n)} \cdot n \cdot \mathscr{D}_n \mathbf{B}^{(n)} = \mathscr{D}_n \mathbf{A}^{(n)} \cdot n \cdot \mathbf{B}^{(n)} \tag{7}$$

Theorem 2.7. *If* $\mathbf{A}^{(n)}$ *is a traceless totally symmetric tensor, then* $\mathscr{D}_n \mathbf{A}^{(n)} = (2n-1)!!\mathbf{A}^{(n)}$.

Corollary 2.8. *If* $\mathbf{A}^{(n)}$ *is a totally symmetric tensor and* $\mathbf{B}^{(n)}$ *is a traceless totally symmetric tensor then*

$$\mathbf{A}^{(n)} \cdot n \cdot \mathbf{B}^{(n)} = \frac{1}{(2n-1)!!} \mathscr{D}_n \mathbf{A}^{(n)} \cdot n \cdot \mathbf{B}^{(n)} \tag{8}$$

Proof

$$\begin{aligned} \mathbf{A}^{(n)} \cdot n \cdot \mathbf{B}^{(n)} &= \frac{1}{(2n-1)!!} \mathbf{A}^{(n)} \cdot n \cdot \mathscr{D}_n \mathbf{B}^{(n)} \quad \text{using Theorem2.7} \\ &= \frac{1}{(2n-1)!!} \mathscr{D}_n \mathbf{A}^{(n)} \cdot n \cdot \mathbf{B}^{(n)} \quad \text{using Theorem2.6} \end{aligned} \tag{9}$$

Corollary 2.9. *If* $\mathbf{A}^{(l)}, \mathbf{B}^{(n)}$ *and* $\mathbf{C}^{(m)}$ *are traceless and symmetric tensors* $\{\forall(n,m) : l = n + m\}$ *and* $\mathbf{A}^{(l)} = \sum_{nm} c_{nm} \mathbf{B}^{(n)} \mathbf{C}^{(m)}$ *then*

$$\mathscr{D}_l \mathbf{A}^{(l)} = \sum_{nm} \frac{(2l-1)!!}{(2n-1)!!(2m-1)!!} c_{nm} \mathscr{D}_n \mathbf{B}^{(n)} \mathscr{D}_m \mathbf{C}^{(m)} \tag{10}$$

Proof. Use Theorem 2.7. □

2.5. Maxwell Cartesian tensors

An expression for solid harmonics in terms of the gradient of the position r^{-1} was first derived by Maxwell of an arbitrary set of n axis [24]. In the Cartesian coordinate frame, his expressions reduce to

$$\nabla^n r^{-1} = (-1)^n r^{-2n-1} \mathscr{D}_n \mathbf{r}^n \tag{11}$$

This relationship has been obtained by others [29,33] as well. It has been shown that the components of $\mathscr{D}_n \mathbf{r}^n$ are solid harmonics of degree n. Eq. (11) can be used to compute $\nabla^n r^{-v}$. It can be shown that the following expressions are valid in component form:

$$\begin{aligned} \partial_i \frac{1}{r^v} &= \frac{v}{r^{v-1}} \partial_i \frac{1}{r} \\ \partial_i \partial_j \frac{1}{r^v} &= v \partial_i \frac{1}{r^{v-1}} \partial_j \frac{1}{r} + \frac{v}{r^{v-1}} \partial_i \partial_j \frac{1}{r} \\ \partial_i \partial_j \partial_k \frac{1}{r^v} &= v \partial_i \partial_j \frac{1}{r^{v-1}} \partial_k \frac{1}{r} + v \partial_j \frac{1}{r^{v-1}} \partial_i \partial_k \frac{1}{r} + v \partial_i \frac{1}{r^{v-1}} \partial_j \partial_k \frac{1}{r} + \frac{v}{r^{v-1}} \partial_i \partial_j \partial_k \frac{1}{r} \end{aligned} \tag{12}$$

From the above equation, ∂_i denotes a partial derivative with respect to the component i. It is also evident that this function can be constructed in terms of the traceless tensors of the type defined in (11). Furthermore, while the tensor is *totally symmetric*, it is *not* traceless. While this equation demonstrates the relationship between traceless Cartesian harmonics, it is easier to use

$$\partial_i^{n_1}\partial_j^{n_2}\partial_k^{n_3}\left(\frac{1}{r^v}\right) = (-1)^n r^{-2n-v}\sum_{m_1=0}^{\lfloor\frac{n_1}{2}\rfloor}\sum_{m_2=0}^{\lfloor\frac{n_2}{2}\rfloor}\sum_{m_3=0}^{\lfloor\frac{n_3}{2}\rfloor}(-1)^m\begin{bmatrix} n_1 \\ m_1 \end{bmatrix}\begin{bmatrix} n_2 \\ m_2 \end{bmatrix}\begin{bmatrix} n_3 \\ m_3 \end{bmatrix} \times r^{2m} f(v, n-m-1) x^{n_1-2m_1} y^{n_2-2m_2} z^{n_3-2m_3} \tag{13}$$

to construct the n-fold gradient, where $n = n_1 + n_2 + n_3$, $m = m_1 + m_2 + m_3$, and $f(v,n) = v \times (v+2)\times (v+4)\cdots\times(v+2n)$. It can be readily shown that this definition reduces to that obtained for $v = 1$ [29].

Finally, consider a function $f(\mathbf{r}-\mathbf{r}')$ where $\mathbf{r}$ and $\mathbf{r}'$ are used to denote the location of the observation and source points, respectively. An addition theorem for this function may be obtained using Taylor's expansion. In tensorial form, this is stated as follows:

Theorem 2.10 (Taylor expansion). *The function* $f(\mathbf{r}-\mathbf{r}')$ *can be expressed about the origin using*

$$f(\mathbf{r}-\mathbf{r}') = \sum_{n=0}^{\infty}\frac{(-1)^n}{n!}\mathbf{r}'^n \cdot n \cdot \nabla^n f(\mathbf{r}) \tag{14}$$

where $\mathbf{r} > \mathbf{r}'$.

Proof.

$$\begin{aligned} f(\mathbf{r}-\mathbf{r}') &= f(\mathbf{r}) - \sum_{j=1}^{3} r'_j\partial_j f(\mathbf{r}) + \frac{1}{2!}\sum_{j=0}^{3}\sum_{k=0}^{3} r'_j r'_k \partial_j\partial_k f(\mathbf{r}) + \cdots \\ &= f(\mathbf{r}) - (\mathbf{r}'\cdot\nabla)f(\mathbf{r}) + \frac{1}{2!}(\mathbf{r}'\cdot\nabla)^2 f(\mathbf{r}) + \cdots = \sum_{n=0}^{\infty}(-1)^n\frac{1}{n!}(\mathbf{r}'\cdot\nabla)^n f(\mathbf{r}) \\ &= \sum_{n=0}^{\infty}(-1)^n\frac{1}{n!}\mathbf{r}'^n\cdot n\cdot\nabla^n f(\mathbf{r}) \qquad \square \end{aligned} \tag{15}$$

This theorem gives rise to the following corollary.

Corollary 2.11. *The function* $f(\mathbf{r}-\mathbf{r}')$ *takes the form*

$$f(\mathbf{r}-\mathbf{r}') = \begin{cases} \sum_{n=0}^{\infty}\mathbf{M}^{(n)}\cdot n\cdot\nabla^n f(\mathbf{r}) & \text{for } \mathbf{r} > \mathbf{r}' \\ \sum_{n=0}^{\infty}\mathbf{r}^n\cdot n\cdot\mathbf{L}^{(n)} & \text{for } \mathbf{r}' > \mathbf{r} \end{cases} \tag{16}$$

where $\mathbf{M}^{(n)}$ *and* $\mathbf{L}^{(n)}$ *are the multipole and local expansions.*

This formula is the foundation of fast methods that will be proposed in the next section. As an aside, it is interesting to note that an application of this theorem readily leads to an equivalence between Cartesian harmonics and spherical harmonics. Consider $f(\mathbf{r}-\mathbf{r}') = R^{-1}$ where $R = |\mathbf{R}| = |\mathbf{r}-\mathbf{r}|'$. Using Theorem 2.10 and (11), one can readily arrive at

$$\begin{aligned} R^{-1} &= \sum_{n=0}^{\infty}\frac{(-1)^n}{n!}\mathbf{r}'^n\cdot n\cdot\nabla^n r^{-1} = \sum_{n=0}^{\infty}\frac{1}{n!}r^{-2n-1}\mathbf{r}'^n\cdot n\cdot\mathscr{D}_n\mathbf{r}^n = \sum_{n=0}^{\infty}\frac{1}{n!}\frac{r'^n}{r^{n+1}}\hat{\mathbf{r}}'^n\cdot n\cdot\mathscr{D}_n\hat{\mathbf{r}}^n \\ &= \sum_{n=0}^{\infty}\frac{r'^n}{r^{n+1}}P_n(\hat{\mathbf{r}}'\cdot\hat{\mathbf{r}}) \end{aligned} \tag{17}$$

The above equation is immediately recognizable as being equivalent to an expansion in terms of Legendre polynomials $P_n(\cdot)$, and provides the required equivalence between traceless Cartesian tensors and Legendre polynomials (see references in [26] for more details). In the next two sections, we will use some of these ideas to develop fast methods for potentials of the form R^{-v}.

3. Fast evaluation of potentials of the form R^{-v}

3.1. Divide and conquer strategy

Typically, potentials are evaluated between source and observation pairs that are randomly distributed in a domain $\Omega \subset \mathbb{R}^3$. The computational scheme developed here will follow those typically used in FMM. To this end, the entire domain is embedded in a fictitious cube that is then divided into eight sub-cubes, and so on. This process continues recursively until the desired level of refinement is reached; an N_l-level scheme implies $N_l - 1$ recursive divisions of the domain. At any level, the (sub)domain that is being partitioned is called the *parent* of all the eight *children* that it is being partitioned into. At the lowest level, all source/observers are mapped onto the smallest boxes. This hierarchical partitioning of the domain is referred to as a regular oct-tree data structure. The interactions between all source and observation points are now computed using traversal up and down the tree structure. This is done using the following rule: at any level in the tree, all boxes/subdomains are classified as being either in the near or far field of each other using the following dictum: two subdomains are classified as being in the far field of each other if the distance between the centers is at least twice the sidelength of the domain, *and* their parents are in the near field of each other. Once, the interaction list have been built for all levels, the computation proceeds as follows; at the lowest level, interaction between the elements of boxes that are in the nearfield of each other is computed directly, i.e., using $1/R^v$. All other interactions are computed using a three stage algorithm: (i) compute multipoles of sources that reside in each box; (ii) convert these to local expansion at all boxes that are in its far field; (iii) from the local expansion, compute the field at each observer. It is apparent that one can gain more efficiency by embedding this scheme within itself. That is, if two domains that interact with each other are far away, then these clusters may be combined to form larger clusters that then interact with each other at a higher level and so on. As will be shown later, this computational strategy considerably mitigates the overall cost. To accomplish these tasks, it is necessary to develop theorems that enable the following: (i) computation of multipoles at leaf (or smallest boxes); (ii) theorems to shift the origins of multipole so that effects of small clusters can be grouped together to form larger clusters; (iii) translate multipole expansion to local expansion; (iv) move the origin of local expansion so that expansions at the origin of the parent may be disaggregated to those of its children; (v) finally, aggregate the local expansions in a box to compute the field at all the observers. This sequence of tasks are generally referred to as moving up, across, and down the tree, and is facilitated by the theorems developed next.

3.2. General statement of the problem

Consider a domain $\Omega_s \in \mathbb{R}^3$ that is populated with k sources and a domain $\Omega_o \in \mathbb{R}^3$ that contains k observers. With no loss of generality, assume that these domains are spherical and of radius a. These spherical domains completely enclose one of the cubical subdomains generated earlier. The location of these points is random, however we will assume that the distribution in the domain is sufficiently dense and relatively uniform. Centers of Ω_s and Ω_o are denoted by $\mathbf{r}_s$ and $\mathbf{r}_o$. It is assumed that $\Omega_s \subset \overline{\Omega}_s$ and $\Omega_o \subset \overline{\Omega}_o$ and $\overline{\Omega}_s \cap \overline{\Omega}_o = \emptyset$. In what follows, the domains $\overline{\Omega}_s$ and $\overline{\Omega}_o$ will be called parents of Ω_s and Ω_o, respectively. The parent domains will be assumed to be spherical of size $2a$, and their center are denoted by $\mathbf{r}_s^p$ and $\mathbf{r}_o^p$, respectively. The potential due to sources $\forall \mathbf{r}_i \in \Omega_s$ observed at $\mathbf{r} \in \Omega_o$ is given by

$$\phi(\mathbf{r}) = \sum_{i=1}^{k} \frac{q_i}{|\mathbf{r} - \mathbf{r}_i|^v} = \sum_{i=1}^{k} \sum_{n=0}^{\infty} (-1)^n \frac{q_i}{n!} \mathbf{r}_i^n \cdot n \cdot \nabla^n \frac{1}{r^v} = \sum_{n=0}^{\infty} \sum_{i=1}^{k} (-1)^n \frac{q_i}{n!} \mathbf{r}_i^n \cdot n \cdot \nabla^n \frac{1}{r^v} \tag{18}$$

This equation is derived using Theorem 2.10, and q_i are values of the sources at locations $\mathbf{r}_i$. The exchange of the summation indices is permissible as the summation converges. Unless otherwise stated, the operator ∇ operates on $\mathbf{r}$. In what follows, we will prescribe the means that will enable that rapid computation of (18). The presentation will be in two stages: (i) We will develop expressions for computing these using totally symmetric tensors. In this algorithm, the operations for traversing up and down the tree are "exact," i.e., once the multipole or local tensor is known at an origin, shifting the origin is exact. (ii) We will develop another method that relies on cascaded Taylor's series expansion. Here, traversal up and down the tree is not exact. However, in our presentation, we will specialize this technique for $v = 1$ so as to cast it in terms of traceless tensors. Consequently, the resulting algorithm is optimal in the number of operations. With absolute lack of imagination the two techniques will be referred to as methods 1 and 2. The error bounds of method 1 is derived as is the computational cost of both methods. We also give insights into how these methods can be implemented. Parenthetically, we note that in both methods, the v dependence exists only when traversing across the tree.

3.3. Method 1: Cartesian expansions with totally symmetric tensors

Theorem 3.1 (Multipole expansion). *The total potential at any point $\mathbf{r} \in \Omega_o$ due to k sources $q_i, i = 1, \ldots, k$ located at points $\mathbf{r}_i \in \Omega_s$ is given*

$$\begin{aligned}\phi(\mathbf{r}) &= \sum_{n=0}^{\infty} \mathbf{M}^{(n)} \cdot n \cdot \nabla^n \frac{1}{r^v} \\ \mathbf{M}^{(n)} &= \sum_{i=1}^{k} (-1)^n \frac{q_i}{n!} \mathbf{r}_i^n\end{aligned} \tag{19}$$

where $\mathbf{M}^{(n)}$ is the totally symmetric multipole tensor about the origin $\mathbf{r}_s = \{0, 0, 0\}$.

Proof. See (18). □

In the above equations, the tensor $\mathbf{M}^{(n)}$ is of full rank and totally symmetric. This implies that the number of independent components is $(n+1)(n+2)/2$. As we will show in the next subsection, if this tensor is contracted with another tensor that is traceless, then it is possible to use the traceless form of the multipole moment that contains only $2n+1$ independent components.

Next, we present the first addition theorem that enables shifting the origin of multipole expansions centered around $\mathbf{r}_s$ to that centered around $\mathbf{r}_s^p$. This is facilitated by the following theorem. Note, variations of this theorem have been developed in other contexts [29,34].

Theorem 3.2 (Multipole to multipole expansion). *Given a multipole expansion of k sources about the* $\mathbf{r}_s = \{0, 0, 0\}$

$$\mathbf{O}^{(n)} = \sum_{i=1}^{k} (-1)^n \frac{q_i}{n!} \mathbf{r}_i^n \tag{20a}$$

then the multipole expansion about the point $\mathbf{r}_s^p$ can be expressed in terms of (20a) *as*

$$\mathbf{M}^{(n)} = \sum_{i=1}^{k} (-1)^n \frac{q_i}{n!} (\mathbf{r}_i - \mathbf{r}_s^p)^n = \sum_{m=0}^{n} \sum_{P(m,n)} \frac{m!}{n!} (\mathbf{r}_s^p)^{n-m} \mathbf{O}^{(m)} \tag{20b}$$

Proof. Using (19), Theorems 2.1, 2.10 and noting that the tensors $\mathbf{O}^{(n)}$ and $\nabla^n r^{-v}$ are totally symmetric, results in

$$\begin{aligned}\phi(\mathbf{r}) &= \sum_{n=0}^{\infty} \left\{ \sum_{i=1}^{k} (-1)^n \frac{q_i}{n!} (\mathbf{r}_i - \mathbf{r}_s^p)^n \right\} \cdot n \cdot \nabla^n \frac{1}{|\mathbf{r} - \mathbf{r}_s^p|^v} \\ &= \sum_{n=0}^{\infty} \left\{ \sum_{i=1}^{k} (-1)^n \frac{q_i}{n!} \sum_{m=0}^{n} (-1)^{n-m} \sum_{P(n,m)} (\mathbf{r}_s^p)^{n-m} \mathbf{r}_i^m \right\} \cdot n \cdot \nabla^n \frac{1}{|\mathbf{r} - \mathbf{r}_s^p|^v}\end{aligned}$$

$$= \sum_{n=0}^{\infty}\left\{\sum_{m=0}^{n}\sum_{P(n,m)}\frac{m!}{n!}\left(\mathbf{r}_{\mathrm{s}}^{p}\right)^{n-m}\left[\sum_{i=1}^{k}(-1)^{m}\frac{q_i}{m!}\mathbf{r}_i^{m}\right]\right\}\cdot n\cdot\nabla^{n}\frac{1}{|\mathbf{r}-\mathbf{r}_{\mathrm{s}}^{p}|^{\nu}}$$

$$= \sum_{n=0}^{\infty}\left\{\sum_{m=0}^{n}\sum_{P(m,n)}\frac{m!}{n!}\left(\mathbf{r}_{\mathrm{s}}^{p}\right)^{n-m}\mathbf{O}^{(m)}\right\}\cdot n\cdot\nabla^{n}\frac{1}{|\mathbf{r}-\mathbf{r}_{\mathrm{s}}^{p}|^{\nu}} = \sum_{n=0}^{\infty}\mathbf{M}^{(n)}\cdot n\cdot\nabla^{n}\frac{1}{|\mathbf{r}-\mathbf{r}_{\mathrm{s}}^{p}|^{\nu}} \tag{21}$$

where $P(n,m)$ is the permutation of all partitions of n into sets $n-m$ and m. □

Next, we prescribe the means to translate the multipole expansion that exists about $\mathbf{r}_{\mathrm{s}}^{p}$ to a local expansion about $\mathbf{r}_{\mathrm{o}}^{p}$. There are two ways of deriving this translation operator; (i) using reciprocity and (ii) using a Taylor's series expansion. The theorem that is presented next uses the first approach whereas the second approach is used in presenting a similar operation for method 2. As is expected, both result in identical expressions.

Theorem 3.3 (Multipole to local translation). *Assume that the domains $\overline{\Omega}_{\mathrm{s}}$ and $\overline{\Omega}_{\mathrm{o}}$ are sufficiently separated, and the distance between their centers $r_{\mathrm{os}}^{p} = |\mathbf{r}_{\mathrm{os}}^{p}| = |\mathbf{r}_{\mathrm{o}}^{p}-\mathbf{r}_{\mathrm{s}}^{p}|$ is greater that diam$\{\overline{\Omega}_{\mathrm{s}}\}$ and diam$\{\overline{\Omega}_{\mathrm{o}}\}$. If a multipole expansion $\mathbf{M}^{(n)}$ is located at $\mathbf{r}_{\mathrm{s}}^{p}$, then another expansion $\mathbf{L}^{(n)}$ that produces the same field $\forall\mathbf{r}\in\overline{\Omega}_{\mathrm{o}}$ is given by*

$$\begin{aligned}\phi(\mathbf{r}) &= \sum_{n=0}^{\infty}\boldsymbol{\rho}^{n}\cdot n\cdot\mathbf{L}^{(n)}\\ \mathbf{L}^{(n)} &= \sum_{m=n}^{\infty}\frac{1}{n!}\mathbf{M}^{(m-n)}\cdot(m-n)\cdot\tilde{\nabla}^{m}\frac{1}{\left(r_{\mathrm{os}}^{p}\right)^{\nu}}\end{aligned} \tag{22}$$

where $\boldsymbol{\rho} = \mathbf{r}-\mathbf{r}_{\mathrm{o}}^{p}$.

Proof. The potential $\phi(\mathbf{r})\forall\mathbf{r}\in\overline{\Omega}_{\mathrm{o}}$ is given by (19). It follows by reciprocity that if the multipole $\mathbf{M}^{(n)}$ were located at $\mathbf{r}$ it would produce the same potential at $\mathbf{r}_{\mathrm{s}}^{p}$. In other words, the potential at all points $\mathbf{r}\in\overline{\Omega}_{\mathrm{o}}$ can be computed by placing the multipole moments at $\mathbf{r}$ and evaluating

$$\phi(\mathbf{r}) = \sum_{n=0}^{\infty}\mathbf{M}^{(n)}\cdot n\cdot\tilde{\nabla}^{n}\frac{1}{|\mathbf{r}-\mathbf{r}_{\mathrm{s}}^{p}|^{\nu}} \tag{23}$$

at $\mathbf{r}_{\mathrm{s}}^{p}$. Here, $\tilde{\nabla}$ is the derivative with respect to $\mathbf{r}_{\mathrm{s}}^{p}$. Since this valid at all points $\mathbf{r}\in\Omega$, the multipole tensor $\mathbf{M}^{(n)}$ at $\mathbf{r}$ may be translated to the center $\mathbf{r}_{\mathrm{o}}^{p}$. Denoting the multipole tensor at $\mathbf{r}_{\mathrm{o}}^{p}$ by $\mathbf{O}^{(n)}$ and $\boldsymbol{\rho} = \mathbf{r}-\mathbf{r}_{\mathrm{o}}^{p}$, using the multipole expansion theorem, we obtain the potential

$$\begin{aligned}\phi(\mathbf{r}) &= \sum_{n=0}^{\infty}\mathbf{O}^{(n)}\cdot n\cdot\tilde{\nabla}^{n}\frac{1}{\left(r_{\mathrm{os}}^{p}\right)^{\nu}} = \sum_{n=0}^{\infty}\left(\sum_{m=0}^{n}\frac{1}{m!}\boldsymbol{\rho}^{m}\mathbf{M}^{(n-m)}\right)\cdot n\cdot\tilde{\nabla}^{n}\frac{1}{\left(r_{\mathrm{os}}^{p}\right)^{\nu}}\\ &= \sum_{n=0}^{\infty}\sum_{m=0}^{n}\boldsymbol{\rho}^{m}\cdot m\cdot\left(\frac{1}{m!}\mathbf{M}^{(n-m)}\cdot(n-m)\cdot\nabla^{n}\frac{1}{\left(r_{\mathrm{os}}^{p}\right)^{\nu}}\right) = \sum_{n=0}^{\infty}\boldsymbol{\rho}^{n}\cdot n\cdot\mathbf{L}^{(n)}\end{aligned} \tag{24}$$

where

$$\mathbf{L}^{(n)} = \sum_{m=n}^{\infty}\frac{1}{n!}\mathbf{M}^{(m-n)}\cdot(m-n)\cdot\tilde{\nabla}^{m}\frac{1}{\left(r_{\mathrm{os}}^{p}\right)^{\nu}} \tag{25}$$

is obtained by gathering tensors that operate upon $\boldsymbol{\rho}^{n}$. □

Next, we prescribe the means to traverse down from $\mathbf{r}_{\mathrm{o}}^{p}$ to $\mathbf{r}_{\mathrm{o}}$. This theorem is almost a mirror of that used to go up the tree.

Theorem 3.4 (Local to local expansion). *A local expansion $\mathbf{O}^{(n)}$ that exists in the domain $\overline{\Omega}_{\mathrm{o}}$ centered around $\mathbf{r}_{\mathrm{o}}^{p}$ can be shifted to the domain Ω_o centered at $\mathbf{r}_o$ using*

$$\mathbf{L}^{(n)} = \sum_{m=n}^{\infty}\binom{m}{m-n}\mathbf{O}^{(m)}\cdot(m-n)\cdot\left(\mathbf{r}_{o}^{cp}\right)^{m-n} \tag{26}$$

Proof. Starting with the definition of $\phi(\mathbf{r})$, we use $\boldsymbol{\rho} = \mathbf{r} - \mathbf{r}_o + (\mathbf{r}_o - \mathbf{r}_o^p) = \boldsymbol{\rho}_{oi} + \mathbf{r}_o^{cp}$ to obtain

$$\phi(\mathbf{r}) = \sum_{n=0}^{\infty} \mathbf{O}^{(n)} \cdot n \cdot \boldsymbol{\rho}^n = \sum_{n=0}^{\infty} \mathbf{O}^{(n)} \cdot n \cdot (\boldsymbol{\rho}_{oi} + \mathbf{r}_o^{cp})^n = \sum_{n=0}^{\infty} \mathbf{O}^{(n)} \cdot n \cdot \left[\sum_{m=0}^{n} \binom{n}{m} (\mathbf{r}_o^{cp})^{n-m} (\boldsymbol{\rho}_{oi})^m \right] = \sum_{n=0}^{\infty} \mathbf{L}^{(n)} \cdot n \cdot (\boldsymbol{\rho}_{oi})^n \tag{27a}$$

where

$$\mathbf{L}^{(n)} = \sum_{m=n}^{\infty} \binom{m}{m-n} \mathbf{O}^{(m)} \cdot (m-n) \cdot (\mathbf{r}_o^{cp})^{m-n} \qquad \square \tag{27b}$$

In deriving the above proof, we used Theorem 2.1 to permute the tensors, and then gathered terms associated with $(\boldsymbol{\rho}_{oi})^m$ to arrive at the final result. Finally, the potential at any point in the Ω_o can be obtained using

$$\phi(\mathbf{r}) = \sum_{n=0}^{\infty} \mathbf{L}^{(n)} \cdot n \cdot (\boldsymbol{\rho}_{oi})^n \tag{28}$$

3.4. Method 2: Cartesian expansions with cascaded Taylor's series

In the above subsection, the scheme presented relies on the use of totally symmetric tensors, and exact operations to traverse up and down the tree, i.e., once the multipole expansions at the lowest level are known, traversal up the tree is exact. Similarly, once the local expansions are known at a level, traversal down the tree is exact. Alternatively one can derive a fast algorithm that is based on cascaded Taylor's series expansions. In fact, it can be shown that the classical FMM falls into this category as do the algorithms proposed by [16–19,28]. Note also, that for a given error, method 1 will typically require lower value of P than method 2. However, our motivation herein is to demonstrate that for $v = 1$, this algorithm can be formulated in terms of traceless tensors, thus, making the number of operations optimal in the sense of classical FMM. For $v \neq 1$, the translation operator is *not* traceless but a symmetric tensor. Consequently, the asymptotic cost is the same as that of method 1.

3.4.1. Traceless operations for v = 1

As is evident in Theorem 3.1, the multipole tensor is contracted with a tensor that is both totally symmetric *and* traceless. As was mentioned earlier, the latter has only $(2n+1)$ independent components while the former has $(n+1)(n+2)/2$ independent components. However, as was shown in Lemma 2.2, it may well be possible to derive another tensor that results in lower number of operations; here, we develop a method using traceless tensors that are henceforth denoted by a subscript t. The following Lemma demonstrates this fact:

Lemma 3.5 (Traceless multipole). *If the potential at a point is given in terms of contraction between the multipole tensor* $\mathbf{M}^{(n)}$ *and a symmetric traceless tensor, then the same potential at that point may be obtained using an equivalent traceless symmetric tensor* $\mathbf{M}_t^{(n)}$.

Proof. Starting with (19), it follows that

$$\begin{aligned} \phi(\mathbf{r}) &= \sum_{n=0}^{\infty} \mathbf{M}^{(n)} \cdot n \cdot \left[(-1)^n r^{-2n-1} \mathscr{D}_n \mathbf{r}^n \right] \quad \text{From (11)} \\ &= \sum_{n=0}^{\infty} \frac{(-1)^n r^{-2n-1}}{(2n-1)!!} \mathbf{M}^{(n)} \cdot n \cdot \mathscr{D}_n \mathscr{D}_n \mathbf{r}^n \quad \text{From Theorem2.7} \\ &= \sum_{n=0}^{\infty} \frac{1}{(2n-1)!!} \mathscr{D}_n \mathbf{M}^{(n)} \cdot n \cdot [(-1)^n r^{-2n-1} \mathscr{D}_n \mathbf{r}^n] \quad \text{From Theorem2.6} \\ &= \sum_{n=0}^{\infty} \mathbf{M}_t^{(n)} \cdot n \cdot \nabla^n \frac{1}{r} \end{aligned} \tag{29}$$

Next, we need to translate the multipoles located at $\mathbf{r}_{\mathrm{s}}$ to one that is located at $\mathbf{r}_{\mathrm{s}}^{p}$. In contrast to what was done in Theorem 3.2, the starting point of our expansion will be Theorem 3.1. The following lemma prescribes the relation between the traceless tensor $\mathbf{O}_t^{(n)}$ that exists at $\mathbf{r}_{\mathrm{s}}$ to a traceless tensor $\mathbf{M}_t^{(n)}$.

Lemma 3.6 (Traceless multipole to multipole). *A traceless multipole tensor* $\mathbf{O}_t^{(m)}$ *at* $\mathbf{r}_{\mathrm{s}} = (0,0,0)$ *is related to* $\mathbf{M}_t^{(m)}$ *that is centered at* $\mathbf{r}_{\mathrm{s}}^{p}$ *via*

$$\mathbf{M}_t^{(m)} = \sum_{n=0}^{m} \frac{(-1)^n}{n!} \frac{\mathscr{D}_n(\mathbf{r}_{\mathrm{s}}^{p})^n}{(2n-1)!!} \mathbf{O}_t^{(m-n)} \tag{30}$$

Proof. The proof presented herein relies on the repeated use of Theorems 2.6, 2.7, and Corollary 2.8. These theorems essentially permit manipulations of the Detracer operator, as long as one of the tensors involved in the contraction is traceless. As seen in Theorem 3.5, the tensor $\nabla^n r^{-1}$ is traceless, consequently, all quantities that are contracted with it can be made traceless as well. Starting with Lemma 3.5 and using Taylor expansion (Theorem 2.10) results in

$$\begin{aligned}\phi(\mathbf{r}) &= \sum_{n=0}^{\infty} \mathbf{O}_t^{(n)} \cdot n \cdot \nabla^n \frac{1}{r} = \sum_{n=0}^{\infty} \mathbf{O}_t^{(n)} \cdot n \cdot \nabla^n \left[\sum_{k=0}^{\infty} \frac{(-1)^k}{k!} (\mathbf{r}_{\mathrm{s}}^{p})^k \cdot k \cdot \nabla^k \frac{1}{|\mathbf{r}-\mathbf{r}_{\mathrm{s}}^{p}|} \right] \\ &= \sum_{n=0}^{\infty} \sum_{k=0}^{\infty} \mathbf{O}_t^{(n)} \cdot n \cdot \nabla^n \left[\frac{(-1)^k}{(2k-1)!!k!} \mathscr{D}_k(\mathbf{r}_{\mathrm{s}}^{p})^k \cdot k \cdot \nabla^k \frac{1}{|\mathbf{r}-\mathbf{r}_{\mathrm{s}}^{p}|} \right] \\ &= \sum_{n=0}^{\infty} \sum_{k=0}^{\infty} \frac{(-1)^k}{(2k-1)!!k!} \mathbf{O}_t^{(n)} \mathscr{D}_k(\mathbf{r}_{\mathrm{s}}^{p})^k \cdot (n+k) \cdot \nabla^{n+k} \frac{1}{|\mathbf{r}-\mathbf{r}_{\mathrm{s}}^{p}|} = \sum_{m=0}^{\infty} \mathbf{M}_t^{(m)} \cdot m \cdot \nabla^m \frac{1}{|\mathbf{r}-\mathbf{r}_{\mathrm{s}}^{p}|}\end{aligned} \tag{31}$$

where

$$\mathbf{M}_t^{(m)} = \sum_{n=0}^{m} \frac{(-1)^n}{n!} \frac{\mathscr{D}_n(\mathbf{r}_{\mathrm{s}}^{p})^n}{(2n-1)!!} \mathbf{O}_t^{(m-n)} \qquad \square \tag{32}$$

The next stage is the translation of the multipoles $\mathbf{M}_t^{(n)}$ to local expansion. Indeed, the procedure for doing so is similar to the one derived for symmetric tensors.

Lemma 3.7 (Traceless multipole to local). *Assume that the domains* $\overline{\Omega}_{\mathrm{s}}$ *and* $\overline{\Omega}_{\mathrm{o}}$ *are sufficiently separated, and the distance between their centers is* $r_{\mathrm{os}}^{p} = |\mathbf{r}_{\mathrm{os}}^{p}| = |\mathbf{r}_{\mathrm{o}}^{p} - \mathbf{r}_{\mathrm{s}}^{p}|$ *is greater that* $\mathrm{diam}\{\overline{\Omega}_{\mathrm{s}}\}$ *and* $\mathrm{diam}\{\overline{\Omega}_{\mathrm{o}}\}$. *If a traceless multipole expansion* $\mathbf{M}_t^{(n)}$ *for all n is located at* $\mathbf{r}_{\mathrm{s}}^{p}$, *then another expansion* $\mathbf{L}^{(n)}$ *that produces the same field* $\forall \mathbf{r} \in \overline{\Omega}_{\mathrm{o}}$ *is given by* $\phi(\mathbf{r}) = \sum_{n=0}^{\infty} \boldsymbol{\rho}^n \cdot n \cdot \mathbf{L}_t^{(n)}$ *where*

$$\mathbf{L}_t^{(n)} = \sum_{m=n}^{\infty} \frac{1}{n!} \nabla^m \frac{1}{(r_{\mathrm{os}}^{p})^{v}} \cdot (m-n) \cdot \mathbf{M}_t^{(m-n)} \tag{33}$$

Proof. The proof presented in this section relies on using another Taylor expansion to create the traceless local expansion $\mathbf{L}_t^{(n)}$ as opposed to using reciprocity to derive similar operators for Method 1. Following Theorem 3.1, assume that a multipole expansion exists at $\mathbf{r}_{\mathrm{s}}^{p} \in \overline{\Omega}_{\mathrm{s}}$. Using Theorem 3.3, we can write the potential at any point $\mathbf{r} \in \overline{\Omega}$ as

$$\phi(\mathbf{r}) = \sum_{n=0}^{\infty} \mathbf{M}^{(n)} \cdot n \cdot \nabla^n \frac{1}{|\mathbf{r}-\mathbf{r}_{\mathrm{s}}^{p}|} = \sum_{n=0}^{\infty} \mathbf{M}_t^{(n)} \cdot n \cdot \nabla^n \frac{1}{|\mathbf{r}-\mathbf{r}_{\mathrm{s}}^{p}|} \tag{34}$$

Using $\mathbf{r} - \mathbf{r}_{\mathrm{s}}^{p} = \mathbf{r} - \mathbf{r}_{\mathrm{o}}^{p} + (\mathbf{r}_{\mathrm{o}}^{p} - \mathbf{r}_{\mathrm{s}}^{p}) = \boldsymbol{\rho} + \mathbf{r}_{\mathrm{os}}^{p}$, $\tilde{\nabla} = \nabla$ where $\tilde{\nabla}$ denotes a derivative with respect to the $\mathbf{r}_{\mathrm{os}}^{p}$, and Theorems 2.6 and 2.10 we can rewrite the above equation as

$$\begin{aligned}\phi(\mathbf{r}) &= \sum_{n=0}^{\infty}\mathbf{M}_t^{(n)}\cdot n\cdot\nabla^n\frac{1}{|\boldsymbol{\rho}+\mathbf{r}_{\mathrm{os}}^p|} = \sum_{n=0}^{\infty}\mathbf{M}_t^{(n)}\cdot n\cdot\tilde{\nabla}^n\frac{1}{|\boldsymbol{\rho}+\mathbf{r}_{\mathrm{os}}^p|}\\ &= \sum_{n=0}^{\infty}\mathbf{M}_t^{(n)}\cdot n\cdot\tilde{\nabla}^n\sum_{k=0}^{\infty}\left[\frac{1}{k!}\boldsymbol{\rho}^k\cdot k\cdot\tilde{\nabla}^k\frac{1}{r_{\mathrm{os}}^p}\right] = \sum_{n=0}^{\infty}\mathbf{M}_t^{(n)}\cdot n\cdot\tilde{\nabla}^n\sum_{k=0}^{\infty}\left[\frac{1}{k!}\boldsymbol{\rho}_t^k\cdot k\cdot\tilde{\nabla}^k\frac{1}{r_{\mathrm{os}}^p}\right]\\ &= \sum_{n=0}^{\infty}\mathbf{L}^{(n)}\cdot n\cdot\boldsymbol{\rho}_t^n \quad \text{Gathering tensors operating on } \boldsymbol{\rho}_t^n = \sum_{n=0}^{\infty}\mathbf{L}_t^{(n)}\cdot n\cdot\boldsymbol{\rho}_t^n \end{aligned} \tag{35}$$

where

$$\begin{aligned}\boldsymbol{\rho}_t^k &= \frac{1}{(2k-1)!!}\mathscr{D}_k\boldsymbol{\rho}^k\\ \mathbf{L}_t^{(n)} &= \frac{1}{(2n-1)!!}\mathscr{D}_n\mathbf{L}^{(n)}\\ \mathbf{L}^{(n)} &= \sum_{k=n}^{\infty}\frac{1}{n!}\tilde{\nabla}^k\frac{1}{r_{\mathrm{os}}^p}\cdot(k-n)\cdot\mathbf{M}_t^{(k-n)}\\ &= \sum_{k=n}^{\infty}\frac{(-1)^k}{n!}(r_{\mathrm{os}}^p)^{-2k-1}\mathscr{D}_k(\mathbf{r}_{\mathrm{os}}^p)^k\cdot(k-n)\cdot\mathbf{M}_t^{(k-n)} \qquad \square\end{aligned} \tag{36}$$

Next, we prescribe the means to shift the origin of the local expansion from $\mathbf{r}_{\mathrm{o}}^p$ to $\mathbf{r}_{\mathrm{o}}$. This is facilitated by the following Lemma.

Lemma 3.8 (Traceless local to local). *Given a local expansion $\mathbf{O}_t^{(n)}$ that exist in the domain $\overline{\Omega}_{\mathrm{o}}$ centered around $\mathbf{r}_{\mathrm{o}}^p$, it can be shifted to the domain Ω_o centered at $\mathbf{r}_o$ using*

$$\mathbf{L}_t^{(m)} = \sum_{n=0}^{\infty}\binom{m+n}{m}\mathbf{O}_t^{(m+n)}\cdot(m)\cdot\left(\mathbf{r}_o^{cp}\right)_t^n \tag{37}$$

Proof. The process of proving this expansion is similar to what was done for developing the expression for multipole to local translation. The crux of this proof is that all the tensors involved are totally symmetric. The potential at any point $\mathbf{r}\in\Omega_{\mathrm{o}}$ can be written as

$$\begin{aligned}\phi(\mathbf{r}) &= \sum_{n=0}^{\infty}\mathbf{M}_t^{(n)}\cdot n\cdot\tilde{\nabla}^n\left[\sum_{m=0}^{\infty}\frac{1}{m!}(\mathbf{r}-\mathbf{r}_{\mathrm{o}}^c)_t^m\cdot m\cdot\tilde{\nabla}^m\left(\sum_{k=0}^{\infty}\frac{1}{k!}(\mathbf{r}_{\mathrm{o}}^c-\mathbf{r}_{\mathrm{o}}^p)_t^k\cdot k\cdot\tilde{\nabla}^k\frac{1}{r_{\mathrm{os}}^p}\right)\right]\\ &= \sum_{m=0}^{\infty}\sum_{k=0}^{\infty}\binom{m+k}{m}(\mathbf{r}-\mathbf{r}_{\mathrm{o}}^c)_t^m(\mathbf{r}_{\mathrm{o}}^c-\mathbf{r}_{\mathrm{o}}^p)_t^k\cdot(m+k)\cdot\sum_{n=0}^{\infty}\frac{1}{(m+k)!}\tilde{\nabla}^{n+m+k}\frac{1}{r_{\mathrm{os}}^p}\cdot n\cdot\mathbf{M}_t^n\\ &= \sum_{m=0}^{\infty}\sum_{k=0}^{\infty}\binom{m+k}{m}(\mathbf{r}-\mathbf{r}_{\mathrm{o}}^c)_t^m(\mathbf{r}_{\mathrm{o}}^{cp})_t^k\cdot(m+k)\cdot\mathbf{O}_t^{(m+k)}\\ &= \sum_{m=0}^{\infty}(\mathbf{r}-\mathbf{r}_{\mathrm{o}}^c)_t^m\cdot m\cdot\sum_{k=0}^{\infty}\binom{m+k}{m}(\mathbf{r}_{\mathrm{o}}^{cp})_t^k\cdot k\cdot\mathbf{O}_t^{(m+k)} = \sum_{m=0}^{\infty}(\mathbf{r}-\mathbf{r}_{\mathrm{o}}^c)_t^m\cdot m\cdot\mathbf{L}_t^{(m)} \qquad \square\end{aligned} \tag{38}$$

Corollary 3.9. *The fields at all observation points in the finest level can be obtained using*

$$\phi(\mathbf{r}) = \sum_{m=0}^{\infty}(\mathbf{r}-\mathbf{r}_{\mathrm{o}}^c)_t^m\cdot m\cdot\mathbf{L}_t^{(m)} \tag{39}$$

The proof for this statement can be obtained trivially from the last line of the proof for Lemma 3.8.

3.5. Error bounds

Error bounds derived herein will be for Method 1; the estimates for Method 2 can be obtained either by nesting those obtained here or using those in [11]. As was mentioned earlier, the shifting of origin of the multipole expansion is exact as is shifting the origin of the local expansion. This implies that the error primarily comes from two sources; (i) Taylor's expansion to create the multipole expansion at the level that it is being translated, and (ii) conversion to local expansion. We shall deal with both cases separately. In what follows, we will assume that the source/observation spheres are of radius a. Consider an arbitrary constant nth rank tensor, $\mathbf{A}^{(n)}$. Then, the contractions

$$\mathbf{A}^{(n)} \cdot n \cdot \nabla^n \frac{1}{r^v} \leqslant C_n \mathbf{A}^{(n)} \cdot n \cdot \frac{1}{r^{2n+v}} \mathbf{r}^n \tag{40a}$$

$$\mathbf{A}^{(n)} \cdot n \cdot \mathbf{M}^{(n)} \leqslant C_q \frac{1}{n!} \mathbf{A}^{(n)} \cdot n \cdot \mathbf{r}^n_{i,\max} \tag{40b}$$

where C_n and C_q are constants, and $\mathbf{r}_{i,\max}$ is the vector corresponding to the charge that is farthest away from the origin. The proof for (40a) can be derived using (12) or (13). Likewise, the proof for (40b) can be trivially derived. It follows from these expressions that the absolute error in making the multipole approximation may be obtained using

$$\begin{aligned}\epsilon_m &= \left|\phi(\mathbf{r}) - \sum_{n=0}^{P} \mathbf{M}^{(n)} \cdot n \cdot \nabla^n \frac{1}{r^v}\right| = \left|\sum_{n=P+1}^{\infty} \mathbf{M}^{(n)} \cdot n \cdot \nabla^n \frac{1}{r^v}\right| \leqslant \sum_{n=P+1}^{\infty} \left|\mathbf{M}^{(n)} \cdot n \cdot \nabla^n \frac{1}{r^v}\right| \\ &\leqslant \sum_{n=P+1}^{\infty} C_n C_q \frac{1}{r^{2n+v} n!} \left|\mathbf{r}^n_{i,\max} \cdot n \cdot \mathbf{r}^n\right| \leqslant \sum_{n=P+1}^{\infty} C_m \frac{1}{r^{2n+v} n!} \left|(\mathbf{r}_{i,\max} \cdot 1 \cdot \mathbf{r})^n\right|\end{aligned} \tag{41}$$

Using the Cauchy–Schwartz inequality, $\mathbf{r}_{i,\max} \cdot 1 \cdot \mathbf{r} \leqslant |\mathbf{r}_{i,\max}||\mathbf{r}| \leqslant ar$, it follows that

$$\epsilon_m \leqslant \sum_{n=P+1}^{\infty} C_m \frac{1}{r^{n+v} n!} a^n \leqslant \sum_{n=P+1} C_m \frac{1}{r^v (P+1)!} \left(\frac{a}{r}\right)^n = \frac{1}{(P+1)!} \frac{C_m}{r^{v-1}(r-a)} \left(\frac{a}{r}\right)^{P+1} \tag{42}$$

The above error bounds imply that the expansion converges as long as the observation point lies outside the source sphere. But the error bound is far from being tight. Next, the error bounds on truncating the local expansions are derived as follows:

$$\epsilon_l = \left|\sum_{n=P+1}^{\infty} \boldsymbol{\rho}^n \cdot n \cdot \mathbf{L}^{(n)}\right| = \left|\sum_{n=P+1}^{\infty} \boldsymbol{\rho}^n \cdot n \cdot \sum_{m=n}^{\infty} \frac{1}{n!} \mathbf{M}^{(m-n)} \cdot (m-n) \cdot \tilde{\nabla} \frac{1}{(r^p_{\mathrm{os}})^v}\right| \tag{43}$$

Using the same arguments as before, it follows that

$$\epsilon_l \leqslant \sum_{n=P+1}^{\infty} \frac{1}{(P+1)!} C_l a^n a^{m-n} \frac{1}{(r^p_{\mathrm{os}})^{v+n}} = \frac{1}{(P+1)!} \frac{C_l}{(r^p_{\mathrm{os}})^{v-1}(r^p_{\mathrm{os}} - a)} \left(\frac{a}{r^p_{\mathrm{os}}}\right)^{P+1} \tag{44}$$

The errors incurred in traversing up and down the tree depends on both the multipole and local errors. Eqs. (41) and (43) imply that the approximations converge $\forall v \in \mathbb{R}$, and may be used to develop estimates for the number of harmonics necessary for a given error criterion. These bounds may also be used to develop estimates for the relative error. Fig. 1 plots the predicted relative error for different values of P for interaction between two domains of radius a whose centers are separated by $4a$. The values of v chosen for this demonstration are those that are used in the numerical results section as well. The salient facts evident from Fig. 1 are: (i) the expansions converge for all v with increasing P, and (ii) the expansions converge faster for $v < 0$ than for $v > 0$. Both these fact are borne out in numerical experiments in Section 4. On a slightly different note, *relative* error bounds derived here do not depend on the number of levels in the tree as no error is accrued in traversing either up or down the tree. The multipole (or local) error at

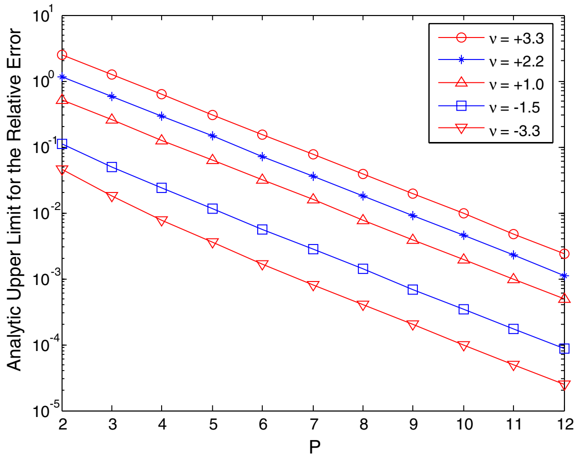

Fig. 1. Analytically derived upper bound for the error for different values of v for source/observation domains of radius a whose centers are separated by 4a.

any two levels in the tree are approximately the same due to the fact that both the distance r and the size of the box a at any level are scaled by the same factor with respect to the smallest box, and this factor drops out.

3.6. Computational methodology, cost, and implementation details

3.6.1. Computational methodology and cost

As mentioned earlier, the entire computational domain is embedded in a cubical domain that is recursively partitioned into smaller cubes. Both near and far interaction lists are created at all levels. In what follows, we describe the computational methodology as well as the cost associated with each operation. The cost associated will be denoted by C^{i}_{op} where $i = 1, 2$ denotes the method used and op denotes the specific operation. It is to be noted that the cost C^{2}_{op} is specifically for $v = 1$. If Method 2 were to be used for evaluating potentials for $v \neq 1$, i.e., use cascaded Taylor expansion, then the cost would be identical to that of Method 1 for all stages of the operations. This is a result of the fact that the tensors for $v \neq 1$ are not traceless. The operations $\mathrm{op} \in \{\mathrm{NF}, \mathrm{C2M}, \mathrm{M2M}, \mathrm{M2L}, \mathrm{L2L}, \mathrm{L2O}\}$ that stand for (i) near field, (ii) charge to multipole, (iii) multipole to multipole, (iv) multipole to local, (v) local to local, and (vi) local to observer. In what follows, we will denote the total number of interaction points by N, the number of harmonics by P, the number of levels in the tree by N_l and the number of boxes at any level by $N_{\mathrm{b},l}$. It will be assumed that the interaction points are uniformly distributed in a volume. We will also assume that the number of unknowns in each leaf box is s. It follows that $N_{\mathrm{b},1} = N/s, N_{\mathrm{b},l-1} = 8N_{\mathrm{b},l}$, and $\sum_{i=1}^{N_l} N_{\mathrm{b},i} \propto N/s$. With these preliminaries, the computational methodology can be prescribed as follows:

(1) *Near field evaluation:* At the leaf level, all boxes that lie in the near field are tabulated. This implies that one computes the interaction between the points that are in the vicinity of each classically. Therefore, $C^{1}_{\mathrm{NF}} = C^{2}_{\mathrm{NF}}$, and

$$\begin{aligned} C^{1}_{\mathrm{NF}} &\propto \text{Total no. boxes} \times \text{Cost of interaction of each box with its near field} \propto N/s \times 27s^2 \\ &\propto 27Ns \end{aligned} \tag{45}$$

(2) *Far field evaluation:* The far field evaluation comprises of four operations.

(a) *Multipole expansion*: For all boxes at the lowest level, compute the multipole expansion for all charges that reside in it. This is done using Theorem 3.1 for method 1 or Lemma 3.5 for method 2. The former forms a set of totally symmetric tensors whereas the latter forms traceless tensors. The cost for this operation is

$$C^i_{\mathrm{C2M}} \propto \text{total no of level 1 boxes} \times \text{Cost for each box}$$
$$\propto \text{total no of level 1 boxes} \times \text{no. charges per box}$$
$$\times \text{cost per tensor} \times \text{no of tensors}$$

$$\begin{aligned} C^1_{\mathrm{C2M}} &\propto \frac{N}{s} \times s \times \sum_{p=0}^{P} (p+1)(p+2)/2 \\ &\propto \left(\frac{N}{6} P^3\right) \\ C^2_{\mathrm{C2M}} &\propto \frac{N}{s} \times s \times \sum_{p=0}^{P} (2p+1) \\ &\propto NP^2 \end{aligned} \tag{46}$$

(b) *Multipole to multipole*: For all boxes, at any given level, compute the multipole expansion for the parent box from those of its children. This operation is repeated at all levels. As with the classical FMM, the number of operations is independent of child/parent levels. The cost for obtaining a term in the nth rank multipole tensor scales as $(m-n+1)(m-n+2)/2)$ for $m = n, \ldots, P$. Given that there are $(n+1)(n+2/2$ independent terms in nth rank tensor, the cost for constructing all terms of the tensor scales as

$$\begin{aligned} \text{Cost child multipole to parent multipole}^1 &= \sum_{n=0}^{P} (n+1)(n+2)/2 \sum_{m=n}^{P} (m-n+1)(m-n+2)/2 \\ &= \prod_{i=1}^{6} \frac{(P+i)}{i} \end{aligned} \tag{47a}$$

The number of operations specified in this equation is exact and exploits the total symmetry of the tensors involved. Similarly, the number of operations required when using traceless tensors is

$$\begin{aligned} \text{Cost child multipole to parent multipole}^2 &= \sum_{n=0}^{P} (2n+1) \sum_{m=n}^{P} (2(m-n)+1) \\ &= \sum_{n=0}^{P} (P-n+1)(P-n-1)(2n+1) \end{aligned} \tag{47b}$$

This implies that the cost

$$C^i_{\mathrm{M2M}} \propto \text{Total number of multipole to multipole translations} \times \text{Cost per translation}$$

$$\begin{aligned} C^1_{\mathrm{M2M}} &\propto \frac{N}{s} \times \prod_{i=1}^{6} \frac{(P+i)}{i} \\ C^2_{\mathrm{M2M}} &\propto \frac{N}{s} \times \sum_{n=0}^{P} (P-n+1)(P-n-1)(2n+1) \end{aligned} \tag{48}$$

(c) *Multipole to local translation*: The cost for translating $P+1$ multipole tensors of one box to local tensors at another is that in (47a) for symmetric tensors and (47b). Consequently, the cost for translation scales as

$$C^i_{\mathrm{M2L}} \propto \text{No. translations per box} \times \text{No of boxes} \times \text{cost for one translation}$$

$$\begin{aligned} C^1_{\mathrm{M2L}} &\propto 189 \frac{N}{s} \prod_{i=1}^{6} \frac{(P+i)}{i} \\ C^2_{\mathrm{M2L}} &\propto 189 \frac{N}{s} \sum_{n=0}^{P} (P-n+1)(P-n-1)(2n+1) \end{aligned} \tag{49}$$

(d) *Local to local translation*: The cost is exactly the same as that for multipole to multipole translation, i.e., $C^1_{\mathrm{L2L}} = C^1_{\mathrm{M2M}}$ and $C^2_{\mathrm{L2L}} = C^2_{\mathrm{M2M}}$.

(e) *Local to observer*: Again, the cost for this operation is exactly the same as that for mapping charge to multipoles, i.e., $C^1_{\mathrm{L2O}} = C^1_{\mathrm{C2M}}$ and $C^2_{\mathrm{L2O}} = C^2_{\mathrm{C2M}}$.

The above analysis implies that the cost for the total analysis scales as

$$\begin{aligned} C^i_{\mathrm{cost}} &= C^i_{\mathrm{NF}} + C^i_{\mathrm{C2M}} + C^i_{\mathrm{M2M}} + C^i_{\mathrm{M2L}} + C^i_{\mathrm{L2L}} + C^i_{\mathrm{L2O}} \quad \text{for } i = 1,2 \\ C^1_{\mathrm{cost}} &\propto 27Ns + 191\frac{N}{s}\frac{P^6}{720} + \frac{NP^3}{3} \\ C^2_{\mathrm{cost}} &\propto 27Ns + 191\frac{N}{s}\frac{P^4}{2} + 2NP^2 \end{aligned} \tag{50}$$

It is readily apparent that the optimal number of unknowns per box is $s \propto P^3/10$ for method 1, and $s \propto P^2$ for method 2. Existing methods for $R^{-\nu}$ [18,19] do not use symmetry in their formulations. Consequently, their translation cost *does not* have a factor of 1/720, and their cost will be more expensive for a given value of P. Given that the cost reduction is a consequence of symmetric tensors, the application of method 2 to $R^{-\nu}$ will have identical cost as method 1. The application of method 2 to R^{-1} results in a complexity that is very similar to that of the classical FMM algorithm that was presented in [11] with an exception of a factor of 1/2 in the translation term. However, recent improvements to the classical FMM scheme have reduced the P^4 scaling to P^3 by using a plane wave based translation operator [14]; using a plane wave based translation operator has enabled some algorithmic changes that have further reduced the "cost in front." Similar modifications to method 2 are possible for $\nu = 1$.

3.7. Implementation subtleties

Two issues stand out when implementing this algorithm; (i) the nth rank operators used for multipole to multipole translation from level $l \to l+1$ and those used for doing the same from level $l+1 \to l+2$ differ by a multiplicative constant; (ii) similarly, the nth rank translation operator for translation of multipole from level $l \to l+1$ and that used for translating multipoles from $l+1 \to l+2$ are related by a constant. Both these statements can be proven by examining the explicit forms of the operators involved. These facts imply that these operators need to be constructed and stored only for boxes at the lowest level and all others can be readily obtained by the operations listed above.

It is also evident that the key component of the cost equation is the number of translations and the number of operations necessary to compute each translation. Some modifications that were originally suggested in [14] can be adapted to this algorithm. Indeed, since the error in shifting the multipole expansion is negligible, one can cluster translations to further reduce the total number of translations. Furthermore, one can exploit the structure of the tensor contractions involved in translation. Some of these improvements have already had a positive impact on the speed of the resulting code [35].

Finally, as with all tree codes (and FMM), the algorithm may be made adaptive in terms of the number of the tensors used, with very little loss in precision. For example, at higher levels in the tree (which correspond to interactions that are further away in space), one could reduce P as the potential is dominated by interactions that are closer. However, in the results presented herein, this is not done. Finally, while the resulting power series expansion is convergent, a concern is the numerical stability of the resulting series. It will be evident in Section 4 that for the range of P, s and ν, this is not a concern. However, further insights into the behavior of the series can be gleaned from (13), and using this expression to compute higher order derivatives yields stable results.

4. Results

In this section, we will demonstrate the validity of the numerical method presented via numerous examples. The overarching goals of this section are as follows: (i) numerically show that the traversal up and down the tree can be performed exactly, (ii) demonstrate that the proposed method produces accurate results for different values of v, (iii) demonstrate that this scheme can be used seamlessly for computing potentials that are superposition of potential of the form R^{-v} for multiple values of v using a single tree traversal, and (iv) experimentally demonstrate that the proposed scheme scales as $\mathcal{O}(N)$. In all experiments, the error will be computed using the following:

$$L_2 = \sqrt{\frac{\sum_i (\phi_{\text{num}}(\mathbf{r}_i) - \phi_{\text{exact}}(\mathbf{r}_i))^2}{\sum_i \phi^2_{\text{exact}}(\mathbf{r}_i)}} \tag{51}$$

As is commonly done, all near field interactions are ignored. This gives us a measure of the error produced by the multipole representation. All timing runs are performed on a Linux desktop that has a 2.8 GHz Intel processor, and the run times reported are obtained using an intrinsic function *dtime*. Finally, P will denote the maximum rank of the tensor used in expansions.

First, we will demonstrate the accuracy of operators used to traverse up and down the tree. The geometric configuration analyzed is as follows: 8000 source/observers populate a cube of dimension $4 \times 4 \times 4$. Of these, 4000 are located at $\Omega_1 = (0.0, 1.0) \times (0.0, 1.0) \times (0.0, 1.0)$, and the rest are located in $\Omega_2 = (3.0, 4.0) \times (3, 0, 4.0) \times (3.0, 4.0)$. The distribution of the points is uniformly random, i.e., the distribution in the domain is almost uniform. This arrangement ensures that following; particles in Ω_1 and Ω_2 interact with each other at level 3. For a given P, the error bound for this interaction can be computed. As we increase the number of levels, the change in the error norm can be attributed solely to the error multipole-to-multipole and local-to-local translations. Table 1 documents the error obtained for different values of P and different levels (while we have data for all 10 levels, only some are presented). All computations are carried out for $v = 2.2$. As is evident from the results presented, the variation of the error obtained from using different levels in the tree is accurate to double precision. Next, we perform a similar experiment, but for the lattice gas potential ($\phi(\mathbf{r}) = \sum_i q_i \ln\{|\mathbf{r} - \mathbf{r}_i|\}$) that is very commonly used in the electronic structure calculations. Again, as is evident from Table 2, the variation of errors for different levels is within double precision accuracy. Note, the translation operator for this function can be readily derived from the material presented earlier.

In the next series of numerical experiment, we demonstrate the efficiency and convergence of the proposed method. This is done by analyzing potentials due to randomly distributed sources at random observation points. In what follows, the source/observation points are co-located, and are randomly distributed. Four different computational domains are chosen: $(0.0, 1.0)^3$, $(0.0, 2.0)^3$, $(0.0, 4.0)^3$ and $(0.0, 8.0)^3$. These domains are populated with 500, 4000, 32,000, and 256,000 source/observers. As mentioned earlier, the size of the smallest box Ω_0 depends on the degree of approximation P. This implies that the number of levels in the tree will vary with P. Tables 3–5 demonstrate convergence and speed for $v = 1$, 3.3, −3.3. All errors reported are computed

Table 1
The variation of errors in multipole to multipole and local to local operations with fixed translation error for $v = 2.2$

	$N_l = 3$	$N_l = 5$	$N_l = 7$	$N_l = 10$
$P = 2$	3.268070962493116E−003	3.268070962493099E−003	3.268070962493107E−003	3.268070962493042E−003
$P = 5$	2.866109269813751E−005	2.866109269813507E−005	2.866109269812455E−005	2.866109269808440E−005
$P = 8$	4.207517301400774E−007	4.207517302158528E−007	4.207517301963213E−007	4.207517301868480E−007
$P = 11$	7.470454043399749E−009	7.470454038637677E−009	7.470454030684618E−009	7.470454009643825E−009

Table 2
Variation of errors in multipole to multipole and local to local operations with fixed translation error for computing the lattice gas potential function

	N_l =3	N_l=5	N_l=7
$P = 2$	2.194595063535085E−004	2.194595063534782E−004	2.194595063534947E−004
$P = 5$	2.949087946097283E−007	2.949087945862075E−007	2.949087945902640E−007
$P = 9$	4.696476490009492E−010	4.696476221096208E−010	4.696476168731461E−010
$P = 15$	5.455886813905556E−014	5.453948560581605E−014	5.451163061523909E−014

Table 3
Errors in Coulomb potential ($v = 1$) computed using the proposed scheme and the directly

No. source	P	Ω_0	Levels	Error	T_{Fast}	T_{dir}
500	2	0.25	3	9.383889728802543E−004	9.9999998E−03	2.0000000E−02
4000	2	0.25	4	4.985339577918570E−004	0.1100	2.010
32,000	2	0.25	5	3.973997680645289E−004	1.7500	148.430
256,000	2	0.25	6	3.784618677245141E−004	16.710	10414.19
1,000,000	2	0.25	7	3.6E−004 (est)	72.14	194332.45 (est)
500	6	0.35	3	5.834474875595625E−005	2.9999999E−02	2.0000000E−02
4000	6	0.35	4	1.832900991458556E−005	0.8500000	1.880
32,000	6	0.35	5	1.051430847990692E−005	10.780	141.350
256,000	6	0.35	6	9.205740607568288E−006	93.650	9469.240
4000	13	0.7	3	7.635060722002502E−007	0.7600	1.010
32,000	13	0.7	4	2.840304330201046E−007	24.030	127.490
256,000	13	0.7	5	2.217480629486048E−007	297.080	9253.120
32,000	22	1.0	3	8.349236749350626E−009	57.090	105.440
256,000	22	1.0	4	6.279167576858578E−009	977.80	8988.850

Timing data for the two methods are reported as well.

Table 4
Errors in potential $1/R^{3.3}$ computed using the proposed scheme and directly

No. source	P	Ω_0	Levels	Error	T_{Fast}	T_{dir}
500	4	0.25	3	6.634150584493979E−003	3.9999998E−02	2.9999998E−02
4000	4	0.25	4	4.633100292496714E−003	0.6799999	2.090
32,000	4	0.25	5	3.478008063355080E−003	7.679999	155.5600
256,000	4	0.25	6	3.009871545496196E−003	72.75999	10626.05
4000	10	0.5	4	8.802364554779558E−005	1.170000	1.550
32,000	10	0.5	5	4.384002845526768E−005	20.430	137.240
256,000	10	0.5	6	2.980527001092105E−005	225.350	9549.740
32,000	22	1.0	3	5.803550600029765E−007	56.7500	105.2500
256,000	22	1.0	4	3.983657151956554E−007	979.7199	8981.890

Timing data for the two methods are reported as well.

Table 5
Errors in potential $R^{3.3}$ computed using the proposed scheme and directly

No. source	P	Ω_0	Levels	Error	T_{Fast}	T_{dir}
500	2	0.25	3	7.808229350307999E−003	9.9999998E−03	2.9999998E−02
4000	2	0.25	4	7.991114181824263E−003	0.130	2.020
32,000	2	0.25	5	7.805327383259029E−003	1.700	152.810
256,000	2	0.25	6	7.879062974909005E−003	16.670	10115.84
500	7	0.4	3	1.673554596784708E−006	3.9999999E−02	9.9999998E−03
4000	7	0.4	4	1.204438060165841E−006	0.670	1.760
256,000	7	0.4	6	1.075404282226350E−006	106.1900	9793.580
4000	10	0.6	3	1.201260595754149E−008	1.190	1.340
32,000	10	0.6	4	6.210238339838771E−009	12.650	134.820
256,000	10	0.6	5	5.031536892676515E−009	149.850	9446.090

using (51). As is evident from these tables, the proposed method converges rapidly for different values of v, and is faster than the direct computation. The convergence behavior follows the trends expected for different values of v, as does the timing data with respect to the number of harmonics. Again, as reported earlier, it is possible to choose the size of the smallest box to optimize the timing data; while this is not done precisely here, the size of the smallest box is varied depending on the desired accuracy (P). The breakeven point, of course, depends on the accuracy (and v). For $v = 1$, and $P = 2$ (which results in an error of 10^{-4}), the breakeven point is as low as 250 source/observers. It should be noted that in obtaining this timing data, we have not fully optimized the M2L stage in keeping with some of the development suggested in [14] and in papers thereafter. Even so, the timing data obtained for $v = 1$ and accuracy of 10^{-4} favorably compares with some of the most optimized codes.

Next, we demonstrate the application of this technique to compute the Lennard-Jones potential. The computational domain $\Omega = (0.0, 1.0)^3$ is filled with 12,167 source/observers whose location is uniformly random. The potential computed is of the form $\phi(\mathbf{r}) = q_i(1/R^{12} - 6/R^6)$. A uniform oct-tree with five levels are constructed. As was noted earlier, the traversal up and down the tree are independent of the potential, and *only* the translation across the tree depends on the specifics of the potential being computed. Table 6 tabulates the error with increasing P. As is evident, the potential computed converges rapidly with increasing P.

Finally, we compare the computational cost of the proposed scheme with that of direct computation. Timing data for domains of increasing size are obtained; the number of source/observation pairs vary from 500 to 1,000,000. The density of particles in the domain is chosen to be 500 per unit cube, the particles are randomly distributed in the domain, and $v = -1.5$. The precision $P = \{2, 4, 10\}$, which translates to errors ranging from 10^{-3}, 10^{-6} and 10^{-8}, respectively. In the simulation, the size of the smallest box was kept the same, i.e., $\Omega_0 = 0.25$ for all values of P. All simulations are run on a Linux desktop (running Redhat9.0) with 2.8 GHz Intel Pentium processor with the Intel Fortan compiler. The timing data is obtained using the intrinsic function *dtime*. Fig. 2 compares the time required for computing pairwise potentials classically and using

Table 6
Error in the Lennard-Jones potential; the computations are performed using one tree

P	Error
10	4.614155995813005E−002
14	6.242473037897023E−003
18	3.954018566296799E−004
22	8.407075999784559E−005
32	1.246581347878108E−006

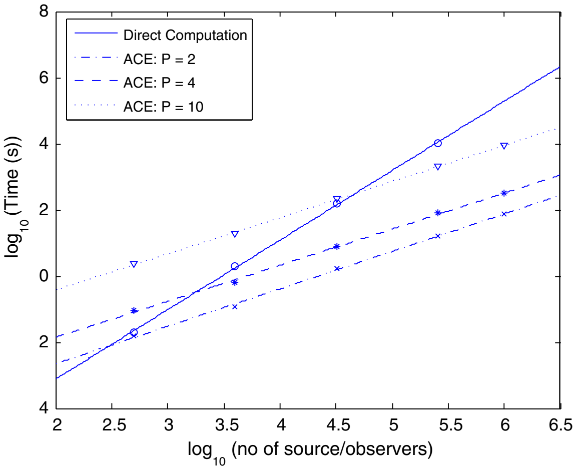

Fig. 2. Cost scaling of the direct method and the fast algorithm (ACE) for different values of the precision P for computing the potential $R^{1.5}$.

the methodology presented herein. It is evident from Fig. 2 that the cost scales as $\mathcal{O}(N)$; the slopes of all three fast methods is approximately 1.0. A noteworthy fact is that the breakeven point, i.e., the number of unknowns above which the proposed technique is computationally more efficient, is as low as 250 source/observation points for an error of 10^{-3}.

5. Summary

In this paper, we have developed two methods for rapidly computing potentials of the form $R^{-\nu}$. Both these methods are founded on addition theorems based on Taylor expansions. Taylor's series has a couple of inherent advantages: (i) it forms a natural framework for developing addition theorem based computational schemes for a range of potentials; (ii) only Cartesian tensors (or products of Cartesian quantities) are used as opposed to special functions. This makes creating a fast scheme possible for potential of the form $R^{-\nu}$. Indeed, it is also possible to generalize the proposed methods to several potentials that are important in mathematical physics [27]. An interesting consequence of the approach has been the demonstration of the equivalence of FMMs that are based on traceless Cartesian tensors to those based on spherical expansions for $\nu = 1$. Finally, we have shown the application of this methodology to computing Coulombic, Lennard-Jones, and lattice gas potentials. We have also demonstrated the efficacy of this scheme for other (non-integer) potential functions. Current research is focused on generalizing the proposed methodology to analyze Yukawa and periodic columbic potentials, retarded and Helmholtz potential for sub-wavelength regimes [35], and fast Gauss transform. Finally, application of is scheme to problems in biophysics, electronic structure calculations, and MD codes are currently underway.

Acknowledgements

We are grateful to NSF for support under CCR-0306436 and to the MSU-IRGP program. We are also grateful to the three anonymous reviewers who went through this document with painstaking thoroughness; the paper has improved significantly thanks in large part to their comments.

References

[1] M.P. Allen, D.J. Tildesley, Computer Simulation of Liquids, Oxford University Press, Oxford, 1987.

[2] R.W. Hockney, J.W. Eastwood, Computer Simulation Using Particles, IOP Publishing, Bristol, 1988.

[3] P. MacNeice, C. Mobarry, K. Olson, Particle-mesh techniques on the maspar, Nasa technical memorandum 104632, NASA, 1996.

[4] H.M.P. Couchman, Mesh-refined p3m: a fast adaptive *n*-body algorithm, Astrophys. J. Lett. 368 (1991) 28.

[5] T. Schlick, Molecular Modeling and Simulation, Springer-Verlag, 2002.

[6] G.H. Kho, W.H. Fink, Rapidly converging lattice sums for nanoelectronic interactions, J. Comp. Chem. 23 (2001) 447–483.

[7] A. Appel, An efficient program for many-body simulations, SIAM J. Sci. Comput. 6 (1985) 85–103.

[8] J. Barnes, P. Hut, A hierarchical $o(n \log n)$ force calculation algorithm, Nature 324 (1986) 446–449.

[9] J.A. Board, W.J. Blamke, D.C. Gray, Z.S. Hukara, W. Elliott, J. Leathrum, Scalable implementations of multipole-accelerated algorithms for molecular dynamics, in: Scalable High Performance Computing Conference, 1994, pp. 87–94.

[10] L. Greengard, V. Rokhlin, A fast algorithm for particle simulations, J. Comput. Phys. 20 (1987) 63–71.

[11] L. Greengard, The Rapid Evaluation of Potential Fields in Particle Systems, MIT Press, Cambridge, MA, 1988.

[12] L. Greengard, W. Gropp, A parallel version of the fast multipole method, Comput. Math. Appl. 20 (1990) 63–71.

[13] L. Greengard, V. Rokhlin, A new version of the fast multipole method for the laplace equation in three dimensions, Acta Numer. 6 (1997) 229–269.

[14] H. Cheng, L. Greengard, V. Rokhlin, A fast adaptive multipole algorithm in three dimensions, J. Comput. Phys. 155 (1999) 468–498.

[15] G.L. Xue, A.J. Zall, P.M. Pardalos, Am. Math. Soc. 23 (1996) 237.

[16] W.D. Elliott, J.A. Board, Technical Report 94-005, Duke Univ Dept EECS. <http://www.ee.duke.edu/research/SciComp/Papers/TR94-005.html> 1994.

[17] M. Fenley, W.K. Olson, K. Chua, A.H. Boschitsch, Fast adaptive multipole method for computation of electrostatic energy in simulations of polyelectrolyte dna, J. Comp. Chem. 17 (1996) 976–991.

[18] Z. Duan, R. Krasny, An adaptive treecode for computing nonbonded potential energy in classical molecular systems, J. Comp. Chem. 22 (2001) 184–195.

[19] I. Chowdhury, V. Jandhyala, Single level multipole expansions and operators for potentials of the form $r^{-\lambda}$, SIAM J. Sci. Comput. 26 (2005) 930–943.

[20] I. Chowdhury, V. Jandhyala, Multilevel multipole and local operators for potentials of the form $r^{-\lambda}$, Appl. Math. Lett. 18 (2005) 1184–1189.

[21] F. Zhao, An $\mathcal{O}(n)$ algorithm for three-dimensional n-body simulation, Master's thesis, Massachusetts Institute of Technology, 1987.

[22] P.B. Visscher, D.M. Apalkov, Charge based recursive fast multipole micromagnetics, Physica B: Phys. Condens. Matter 343 (2004) 184–188.

[23] E.J. Weniger, Addition theorems as three-dimensional Taylor expansions, Int. J. Quant. Chem. 76 (2000) 280–295.

[24] E.W. Hobson, The Theory of Spherical and Ellipsoidal Harmonics, Cambridge University Press, 1931.

[25] T.M. MacRobert, Spherical Harmonics, Dover, 1947.

[26] J. Applequist, Traceless cartesian tensor forms for spherical harmonic functions: new theorems and applications to electrostatics of dielectric media, J. Phys. A: Math. Gen. 22 (1989) 4303–4330.

[27] B. Shanker, H. Huang, Accelerated cartesian expansions–an $\mathcal{O}(n)$ method for computing of non-oscillatory potentials, Technical Report MSU-ECE-Report-2006-06, Michigan State University, 2006.

[28] K. Srinivasan, H. Mahawar, V. Sarin, A multipole based treecode using spherical harmonics for potentials of the form $r^{-\lambda}$, in: Proceedings of the International Conference on Computational Science, Lecture Notes in Computer Science, vol. 3514, Springer-Verlag, Atlanta, Georgia, 2005, pp. 107–114.

[29] J. Applequist, Fundamental relationships in the theory of electric multipole methods and multipole polarizabilities in static fields, Chem. Phys. 85 (1984) 279–289.

[30] J. Applequist, Cartesian polytensors, J. Math. Phys. 24 (1983) 736–742.

[31] R. McWeeny, Symmetry, MacMillan, 1963.

[32] C.G. Grey, K.E. Gubbins, Theory of Molecular Fluids, Clarendon Press, 1984.

[33] E. Buros, H. Bonadeo, Mol. Phys. 44 (1981) 1–15.

[34] A.D. McLean, M. Yashamine, J. Chem. Phys. 47 (1967) 1927.

[35] M. Vikram, B. Shanker, Fast evaluation of time domain fields in sub-wavelength source/observer distributions using accelerated cartesian expansions (ace), Technical Report MSU-ECE-2007-2, Michigan State University.